

# An Ultrathin Five-Band Polarization Insensitive Metamaterial Absorber Having Hexagonal Array of 2D-Bravais-Lattice

Prakash Ranjan<sup>1, \*</sup>, Arvind Choubey<sup>1</sup>, Santosh K. Mahto<sup>2</sup>, and Rashmi Sinha<sup>1</sup>

**Abstract**—In this paper, a novel ultrathin five-band polarization insensitive Metamaterial Absorber (MA) is proposed. The proposed structure consists of a periodic array of six arrows with two concentric hexagonal rings, having novel hexagonal 2D-bravais lattices on a grounded FR-4 dielectric substrate ( $\epsilon_r = 4.25$ , loss-tangent  $\tan \delta = 0.02$ ). The simulated result shows five discrete absorption peaks. The near unity absorption occurs at 2.7, 6.9, 7.3, 13.6 and 16.9 GHz with peak absorptivity of 88.99, 94.45, 87.58, 93.06 and 90.42%, respectively. The proposed absorber is ultrathin with a thickness of  $0.056\lambda_0$  corresponding to the highest frequency of absorption. In order to analyze the absorption mechanism of the structure electromagnetic parameters such as effective permittivity ( $\epsilon_{eff}$ ) and effective permeability ( $\mu_{eff}$ ) are retrieved and plotted. Wave absorption phenomena are explained by comparative tabulation of real and imaginary parts of electromagnetic parameters. Absorption mechanism is further explained by the characteristics impedance and surface current distribution. The structure, being a six-fold symmetric, has been found to be polarization-insensitive under normal incidence. For the oblique incidence of waves, it also achieves high values of absorption for both TE and TM polarizations. The proposed absorber is fabricated, and scattering parameters are measured. Simulated and measured results are in close agreement. Performance of the proposed MA is further investigated by calculating Fractional Bandwidth (FBW). This absorber can find its applications in phase imaging, photo-detector, hyper-spectral imaging, micro-bolometer, spectroscopic detection, surveillance radar and other defence applications.

## 1. INTRODUCTION

Metamaterials being a composite material obtain its unusual electromagnetic properties (negative permittivity, negative permeability etc.) from its unit cell structure have drawn significant interest of researchers in the past decade [1]. It has found many novel applications such as cloaking [2], filters [3], and antennas [4]. After the first proposed Metamaterial Absorber (MA) by Landy et al. in 2008 [5], many such MAs which have single and multiband absorption properties have been proposed [6–12]. MAs have many advantages such as ultra-thin and lightweight compared to conventional absorbers which are bulky and fragile. Although many MAs have been reported earlier, most of them are limited to tri-band, quad-band or penta-band of absorption frequencies [13–17]. Moreover, they all have square packing bravias, hence, there is still lack of sufficient progress towards multiband MAs having more than four absorption frequencies which can be used in phase imaging, photo-detector, hyper-spectral imaging, micro-bolometer, spectroscopic detection, surveillance radar and other defence applications.

In this paper, a novel ultrathin five-band polarization insensitive MA is proposed. The proposed structure consists of a periodic array of two concentric hexagonal rings having hexagonal 2D-bravais lattices on a grounded FR-4 dielectric substrate ( $\epsilon_r = 4.25$ , loss-tangent  $\tan \delta = 0.002$ ). The simulated

---

Received 19 June 2018, Accepted 28 August 2018, Scheduled 9 September 2018

\* Corresponding author: Prakash Ranjan (2014rsec001@nitjsr.ac.in).

<sup>1</sup> Department of Electronics and Communication Engineering, National Institute of Technology, Jamshedpur, India. <sup>2</sup> Department of Electronics and Communication Engineering, Indian Institute of Information Technology, Ranchi, India.

result shows five discrete absorption peaks at 2.7, 6.9, 7.3, 13.6 and 16.9 GHz with a peak absorptivity of 88.99, 94.45, 87.58, 93.06 and 90.42%, respectively. The proposed structure is ultrathin having the thickness of 1 mm, i.e.,  $0.056\lambda_0$  corresponding to the highest absorption frequency. Electromagnetic parameters such as effective permittivity ( $\epsilon_{eff}$ ) and effective permeability ( $\mu_{eff}$ ) are retrieved and plotted to analyze the absorption mechanism of the proposed absorber. Absorption phenomenon is further explained by plotting the characteristics impedance and surface current distribution for all peak absorption frequencies. The structure, being six-fold symmetric, has been found to be polarization-insensitive under normal incidence. It also achieves high absorption for oblique incident angles up to 30 degrees for both TE and TM polarizations. The proposed absorber is fabricated and obtained results found to be in close agreement with the simulated ones. Performance of the proposed MA is further investigated by calculating FBW at all the peak absorption frequencies. The near-perfect absorption component is one of the fundamental building blocks for a phase imaging, photo-detector, hyper-spectral imaging, micro-bolometer and spectroscopic detection, surveillance radar and other defence applications.

## 2. DESIGN OF UNIT CELL STRUCTURE

MA consists of two metallic layers separated by the dielectric substrate as shown in Figure 1. The top layer is FSS (Frequency Selective Surface) which is a periodic metallic unit cell structure whereas bottom layer is ground made of completely covered copper.

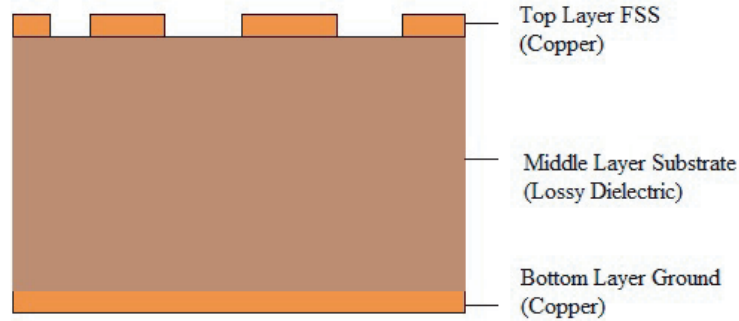


**Figure 1.** Three layer design of MA.

Absorptivity  $A(\omega)$  [9] of the MA can be determined from Equation (1)

$$A(\omega) = 1 - |S_{11}(\omega)|^2 - |S_{21}(\omega)|^2 \quad (1)$$

where  $S_{11}$  and  $S_{21}$  denote reflected and transmitted powers, respectively. Since the bottom layer of MA is completely covered with copper, incident power cannot transmit through it. Therefore, in the absence of transmitted power ( $S_{21} = 0$ ), parameter  $S_{11}$  (Reflection co-efficient) represents the measure of amount of power absorbed by MA. Lesser value of  $S_{11}$  represents more desired absorption of MA.

Most of the proposed metamaterial absorbers have a square array of 2D-bravais lattice with a square geometry of the unit cell [6–18]. Square geometry has lower degree of symmetry than that of hexagonal. Figure 2 illustrates the different degrees of symmetry possessed by unit cell of square and hexagonal geometry. It depicts that square geometry has four-fold symmetry whereas a hexagonal geometry has six-fold symmetry. Higher degree of symmetry leads to more polarization insensitive structure. Hence, a hexagonal geometry with hexagonal 2D-bravais lattice is a suitable candidate for a metamaterial absorber which will provide more polarization insensitivity.

The unit-cell geometry of the proposed structure is shown in Figure 3 with the directions of field vectors (electric field, magnetic field and the direction of incident wave). The structure has two metallic layers (top layer and bottom layer), and both are made of copper (conductivity  $\sigma = 5.8 \times 10^7$  S/m with thickness 0.035 mm) separated by an FR-4 dielectric substrate ( $\epsilon_r = 4.25$ , loss-tangent  $\tan \delta = 0.02$ ) having thickness of 1 mm. The proposed structure consists of a periodic array of six arrows with two concentric hexagonal rings. The bottom surface is completely metal grounded for zero transmission.

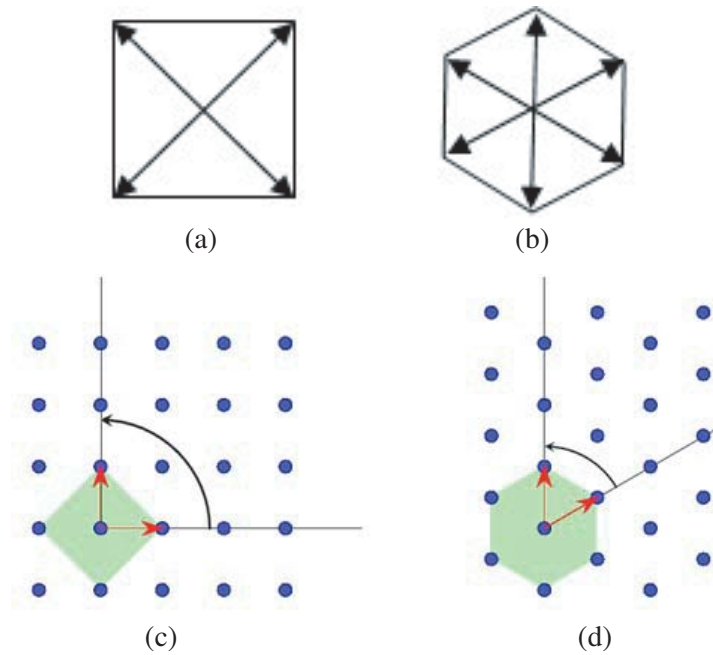


**Figure 2.** (a) Square geometry showing four-fold symmetry, (b) hexagonal geometry showing six-fold symmetry, (c) square 2D-bravais lattice and (d) hexagonal 2D-bravais lattice.

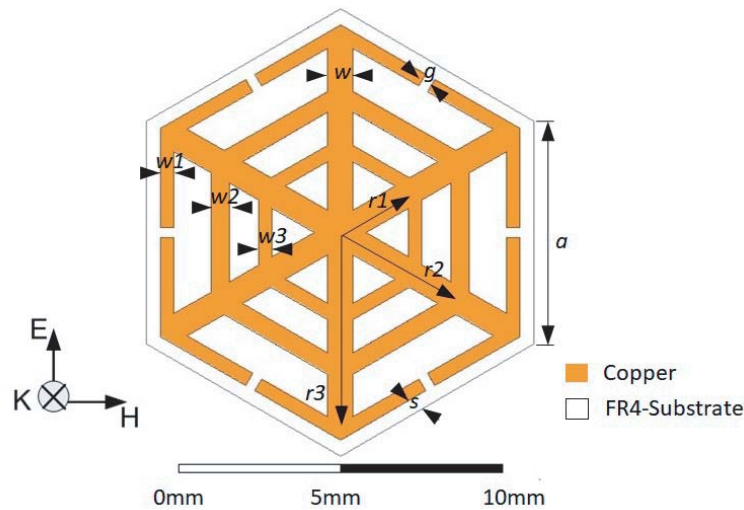


**Figure 3.** Top-view of the unit cell of proposed structure with geometrical dimensions:  $a = 14$  mm,  $s = 1$  mm,  $r1 = 13$  mm,  $r2 = 9.3$  mm,  $r3 = 5.9$  mm,  $w = 1.6$  mm,  $w1 = 1$  mm,  $w2 = 1.4$  mm,  $w3 = 1$  mm and  $g = 0.65$  mm.

### 3. SIMULATION AND ANALYSIS

We performed the simulation of MA using the commercial Ansoft-HFSS. Periodic boundary (Master and Slave boundary) conditions are applied in the  $x$  and  $y$  directions, whereas  $z$ -direction is taken for the electromagnetic wave incident on the MA top surface. The transmission and reflection are obtained from two wave-guide ports (Floquet Ports) placed in front and back of the unit cell.

For the normal incidence of wave, the numerical simulation result is shown in Figure 4 which shows five resonant frequencies at 2.7, 6.9, 7.3, 13.6 and 16.9 GHz with peak absorptivity of 88.99, 94.45, 87.58, 93.06 and 90.42%, respectively.

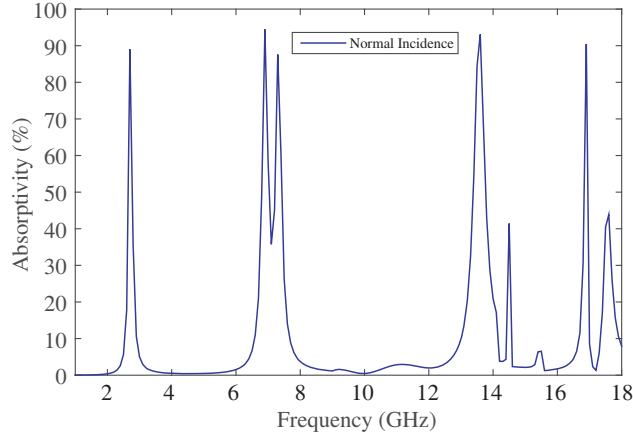


**Figure 4.** Simulated absorptivity of proposed structure.

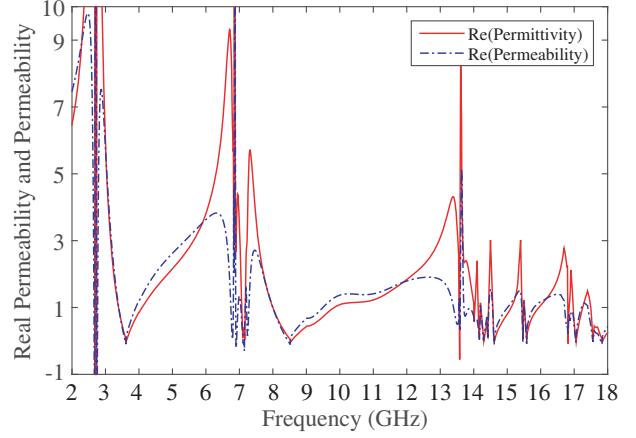


**Figure 5.** Retrieved real part of permittivity and permeability of proposed MA.

Evaluation of effective electromagnetic parameters such as effective permittivity ( $\epsilon_{eff}$ ) and effective permeability ( $\mu_{eff}$ ) can be done by considering metamaterial absorber as a homogeneous medium, thereby applying the formulae given by Smith et al. [19] as:

$$z = \sqrt{\frac{(1 + S_{11})^2 - S_{21}^2}{(1 - S_{11})^2 - S_{21}^2}} \quad (2)$$

$$n = \frac{1}{kd} \cos^{-1} \left[ \frac{1}{2S_{21}} (1 - S_{21}^2 - S_{11}^2) \right] \quad (3)$$

where ‘ $z$ ’ is the impedance, ‘ $n$ ’ the refractive index, ‘ $d$ ’ the thickness of metamaterial absorber, ‘ $k$ ’ the wave number, and ‘ $S_{11}$ ’ & ‘ $S_{21}$ ’ are scattering parameters. These formulas essentially require scattering parameter ‘ $S_{21}$ ’ which is zero in the case of metamaterial absorbers because of having complete metal plate as ground. In order to calculate this, square slots of dimensions  $0.5 \text{ mm} \times 0.5 \text{ mm}$  are cut at the corners of the bottom ground. The slots are cut such that the absorption frequencies do not deviate much from its original values. With ground not completely covered with copper, parameter ‘ $S_{21}$ ’ will be non-zero and can be obtained. The effective value of permittivity and permeability are evaluated through the relationship of reflective index ‘ $n$ ’ and impedance ‘ $z$ ’ as given by

$$\epsilon_{eff} = \frac{n}{z} \quad \text{and} \quad \mu_{eff} = nz. \quad (4)$$

The real and imaginary parts of effective electromagnetic parameters ( $\epsilon_{eff}$  and  $\mu_{eff}$ ) are plotted in Figure 6 and Figure 7, respectively. At peak absorption frequencies  $\epsilon_{eff}$  and  $\mu_{eff}$  change rapidly which shows the electric and magnetic resonances. These changes are such that the normalized impedance becomes equal to unity and contributes in the absorption through impedance transformation. Normalized impedance is given by Equation (5) which reflects that at peak absorption frequencies, real and imaginary parts of  $\epsilon_{eff}$  and  $\mu_{eff}$  are ideally equal to each other. Retrieved values of  $\epsilon_{eff}$  and  $\mu_{eff}$  of the proposed MA are summarized in Table 1. It depicts that at all the five absorption frequencies, real and imaginary parts of  $\epsilon_{eff}$  and  $\mu_{eff}$  are approximately equal to each other, and therefore it explains the phenomenon of high absorption at corresponding five frequencies.

$$z(w) = \sqrt{\frac{\mu_0 \mu_{eff}}{\epsilon_0 \epsilon_{eff}}} = \eta_0 \sqrt{\frac{\mu_{eff}}{\epsilon_{eff}}} \quad (5)$$

$$\text{Normalized Impedance} = \frac{z(w)}{\eta_0} = \sqrt{\frac{\text{Re}(\mu_{eff}) - j\text{Im}(\mu_{eff})}{\text{Re}(\epsilon_{eff}) - j\text{Im}(\epsilon_{eff})}}$$

**Table 1.** Retrieved real and imaginary parts of permittivity and permeability of five band MA.

S. No.	Absorption Frequency (GHz)	Re( $\epsilon_{eff}$ )	Re( $\mu_{eff}$ )	Im( $\epsilon_{eff}$ )	Im( $\mu_{eff}$ )
1	2.72 ( $\approx 2.7$ )	7.59	8.40	54.71	51.32
2	6.87 ( $\approx 6.9$ )	11.30	14.19	9.48	15.38
3	13.62 ( $\approx 13.6$ )	7.87	4.01	9.87	6.80
4	16.8 ( $\approx 16.9$ )	2.22	0.44	4.40	0.70

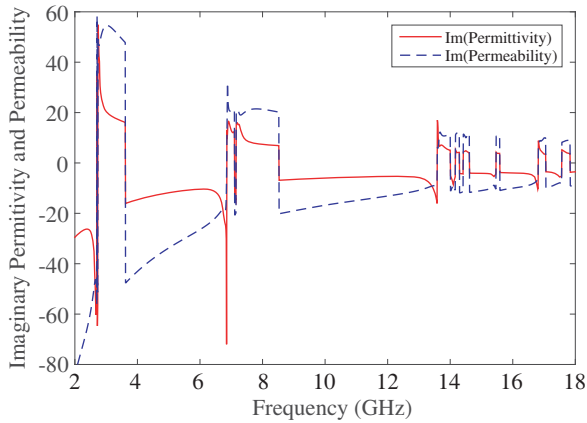


**Figure 6.** Retrieved imaginary part of permittivity and permeability of proposed MA.

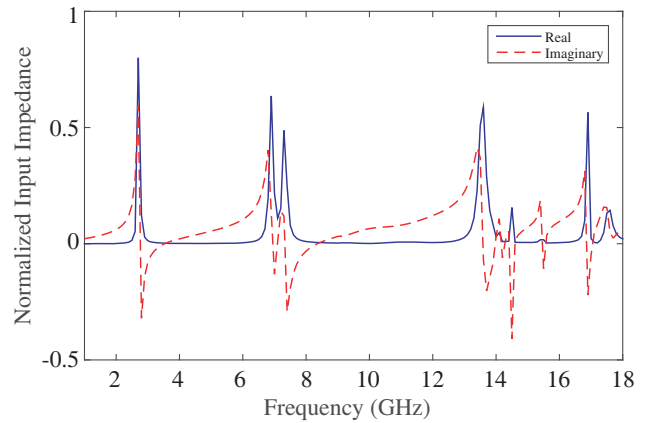


**Figure 7.** Simulated normalized input impedance of proposed MA.

The real and imaginary parts of normalized input impedance are shown in Figure 7. The real part of normalized input impedance has nearly unity value at all the absorption frequencies as imaginary part of normalized input impedance has zero value. This depicts that the impedance of MA is nearly equal to that of free space impedance for incident waves. Hence, incident wave propagates into the MA and gets absorbed. The above structure produces multi-band absorption because different sections of the unit cell structure resonate at different frequencies and thereby achieve multiband absorption even through a single unit cell.

Absorption mechanism of the structure is further analyzed by plotting surface current distribution of the top and bottom surfaces at all the five peak absorption frequencies of the proposed structure, which is shown in Figure 8. The directions of dominant current density at top and bottom layer are anti-parallel to each other forming conduction current (on top and bottom conductors) and displacement current (in between top and bottom layers conductors through dielectric). These conduction and displacement current together forms a current loop at all the peak absorption frequencies. Magnetic excitation occurs due to this circulating current loop as it originates around the incident magnetic field. Electric excitation occurs due to the incident electric field at the top metallic surface. Hence, electric and magnetic excitations occur simultaneously. This is also evident from the very large variation of  $\epsilon_{eff}$  and  $\mu_{eff}$  near all five peak absorption frequencies as shown in Figure 5 and Figure 6. This simultaneous electric and magnetic excitations provide high absorption of incident waves.

The proposed structure of MA has six-fold symmetry, hence it is investigated only up to 30-degree angle of polarization under normal incidence of the wave as shown in Figure 9. It exhibits nearly the same absorption for all polarizations under normal incidence of waves.

The structure is examined under the oblique incidence of a wave for both TE and TM polarizations and obtains simulation results shown in Figure 10 and Figure 11, respectively. Results depict that the absorptivity is still higher (greater than 60%) for a wide angle of oblique incidence of waves (up to 30 degrees) for both the polarizations. The response gets gradually degraded with the increase of incidence

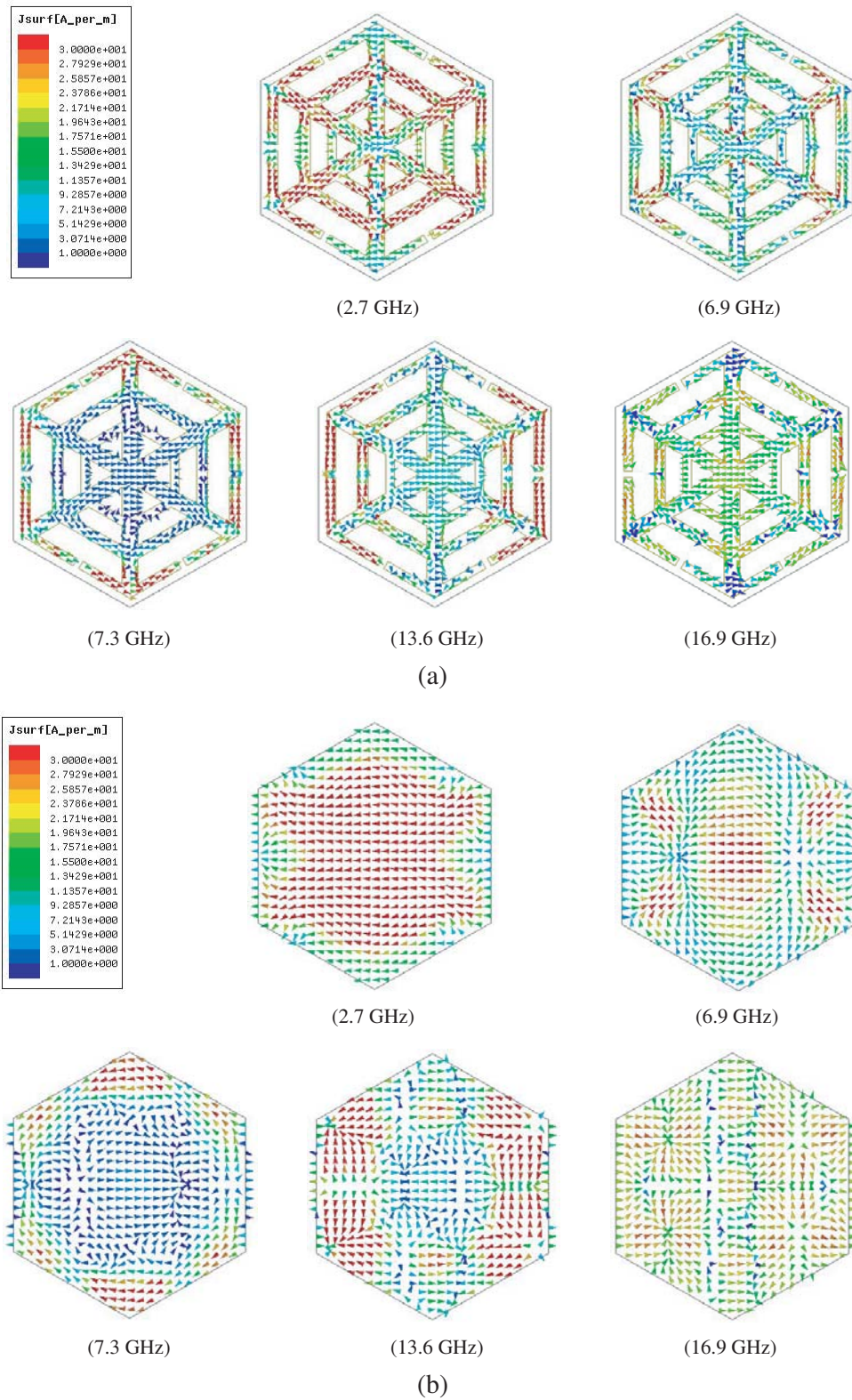


**Figure 8.** Simulated surface current density at (a) top surface and (b) bottom surface of proposed MA.

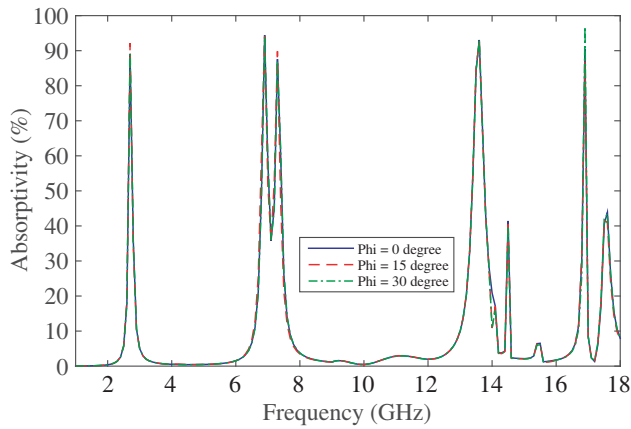


**Figure 9.** Simulated absorption of proposed MA for different polarization angle under normal incidence of waves.

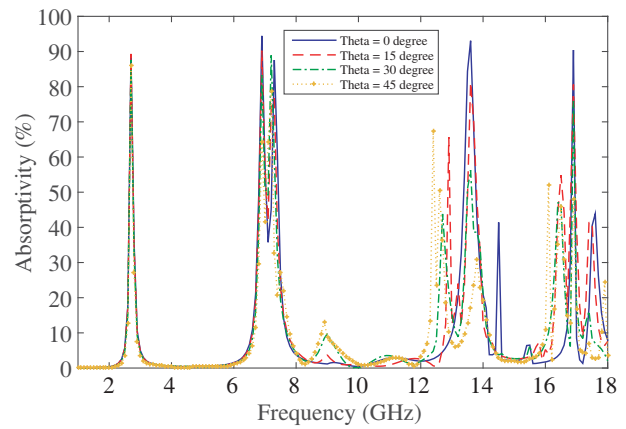


**Figure 10.** Simulated absorption curves of proposed MA for oblique incidence of waves under TE polarization.

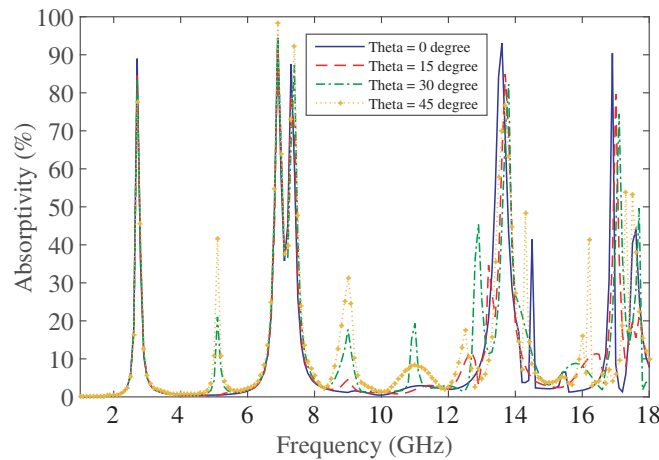


**Figure 11.** Simulated absorption curves of proposed MA for oblique incidence of waves under TE polarization.

angle after 45 degrees of oblique incidence of waves. The detailed description of the experimental setup for measurement of scattering parameter is given in the next section.

#### 4. EXPERIMENTAL RESULTS

The proposed MA is designed and fabricated with readily available substrate FR4 (relative permittivity 4.25). Dimension of each side of the unit cell is 16 mm with thickness 1 mm. As thickness is 0.054 corresponding to the maximum frequency of operation (16.7 GHz), the proposed MPA is ultrathin in nature. An array of  $15 \times 15$  unit cells sample has been fabricated which approximately mimics the infinite periodicity used in the simulation as shown in Figure 12.

The reflection from the fabricated structure is measured inside an anechoic-chamber using two standard horn antennas connected to a vector network analyzer (Anritsu VNA Master MS2038C, 5 kHz to 20 GHz). The experimental setup for measurement is shown in Figure 13 with its schematic diagram. Initially, an identical copper sheet has been placed in the anechoic chamber, and the reflection coefficient from the surface has been measured which will be used as a reference level for all further measurements. Next, the reflection coefficient of the fabricated structure is measured, and the difference between the measured responses and reference level provides the actual reflection from the structure which neglects

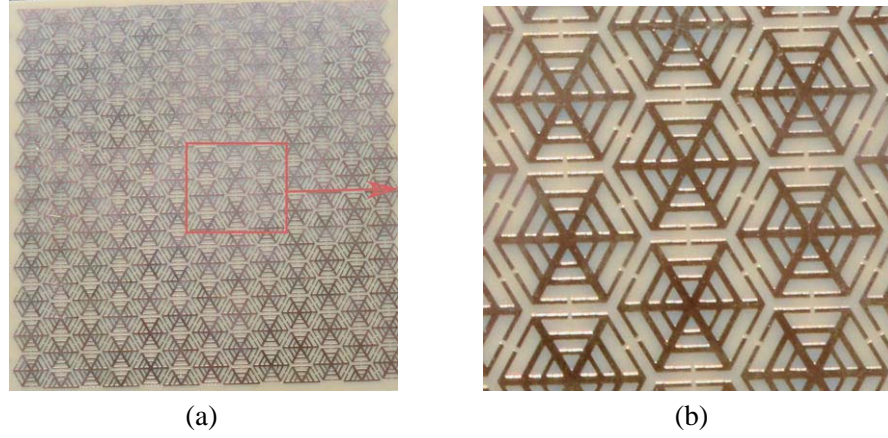


**Figure 12.** Fabricated model of (a) proposed MA along with (b) enlarge view.

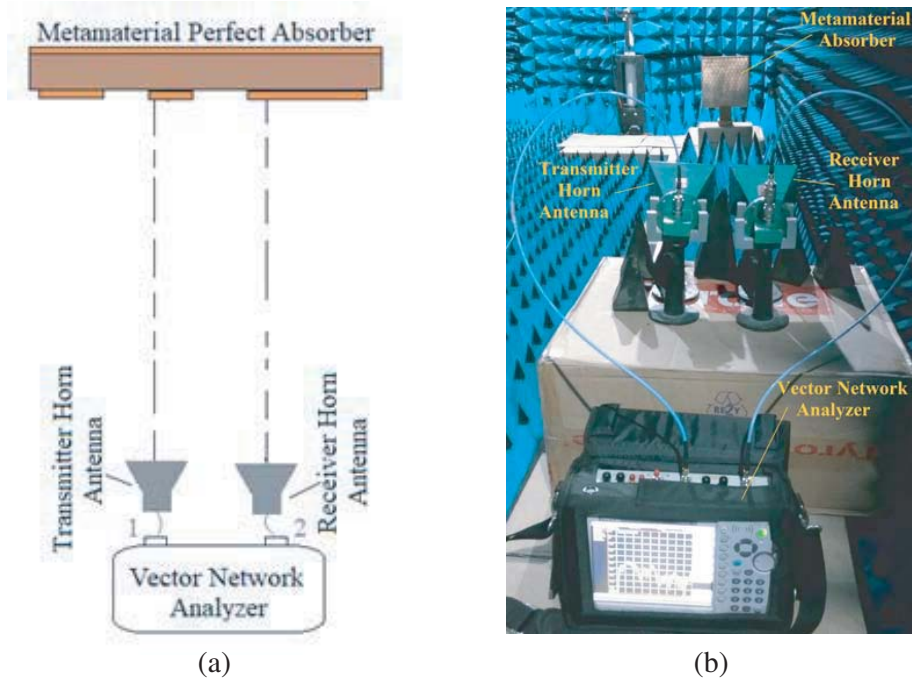


**Figure 13.** (a) Schematics of experimental setup, (b) experimental setup inside of anechoic chamber.

all the surrounding environment effects.

Figure 14 shows the comparison of simulated result with the measured result of reflection coefficient (parameter  $S_{11}$ ) curve under the normal incidence of the wave. The simulation result exhibits five discrete minima of  $-9.582$ ,  $-12.558$ ,  $-9.059$ ,  $-11.590$  and  $-10.188$  dB at 2.7, 6.9, 7.3, 13.6 and 16.9 GHz, respectively; whereas the corresponding measured result shows discrete minima of  $-9.225$ ,  $-12.413$ ,  $-8.923$ ,  $-11.390$  and  $-9.913$  dB at 2.83, 6.81, 7.42, 13.54 and 17.11 GHz, respectively. This shows that the experimental result matches well with that of the simulated one with slight permissible variation due to fabrication tolerances. Performance of the proposed MA can be further illustrated by calculating fractional bandwidth (FBW) which represents the bandwidth of the MA evaluated at maximum absorption frequency. FBW is evaluated by dividing the half power ( $-3$  dB) bandwidth by the central frequency, i.e., obtained by the formula  $FBW = \Delta f / f_0$ , where  $\Delta f$  and  $f_0$  represent the half power bandwidth and the central frequency respectively.

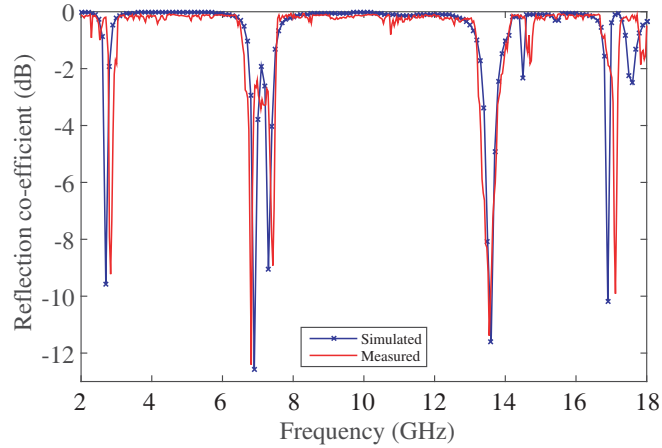


Figure 14. Comparison of simulated result with measured result of reflection co-efficient curve.

Table 2. Simulation and measured FBW of proposed MA.

Simulation			Measurement		
$f_0$ (GHz)	$\Delta f$ (MHz)	FBW (%)	$f_0$ (GHz)	$\Delta f$ (MHz)	FBW (%)
2.7	165	6.11	2.83	140	4.94
6.9	250	3.62	6.81	200	2.93
7.3	225	3.08	7.42	200	2.69
13.6	400	2.94	13.54	585	4.32
16.9	152	0.90	17.11	140	0.81

Table 3. Comparison of proposed absorber with already reported multiband absorbers.

Ref.	Number of Absorption peaks	2D-Lattice Packing	Size of unit cell (mm)	Relative size of unit cell	Thickness (mm)	Relative thickness
[13]	2	Square	10	$0.51\lambda$	0.5	$0.025\lambda$
[14]	3	Square	18	$1.425\lambda$	1	$0.079\lambda$
[15]	4	Square	23	$0.702\lambda$	1	$0.031\lambda$
[16]	4	Square	20	$0.661\lambda$	1.1	$0.037\lambda$
[17]	4	Square	10	$0.504\lambda$	1	$0.050\lambda$
[18]	5	Square	20	$1.039\lambda$	1.5	$0.078\lambda$
Proposed Work	5	Hexagonal	14	$0.788\lambda$	1	$0.056\lambda$

\*  $\lambda$  corresponding to the wavelength of highest absorption frequency.

Table 2 lists the simulated and measured FBWs of the proposed MA. It depicts that absorber has nearly 3% of FBW at four lower peak absorption frequencies which are enough for antenna applications. At the fifth peak absorption frequency, it has nearly 1% of FBW. Hence, this absorber can find some other applications such as phase imaging, photo-detector, hyper-spectral imaging, micro-bolometer, spectroscopic detection, surveillance radar and other defence applications.

The proposed absorber is compared with already reported multiband absorbers as listed in Table 3. Comparisons are done in terms of the number of absorption peaks, 2D-lattice, unit cell size and thickness. As explained earlier, the proposed absorber has a better degree of symmetry design which makes it more polarization insensitive. It has the highest number of absorption peaks and also has comparable unit cell size and thickness.

## 5. CONCLUSION

A novel ultrathin five-band polarization insensitive metamaterial absorber (MA) having novel hexagonal 2D-bravais lattices is proposed. The real and imaginary parts of effective electromagnetic parameters ( $\epsilon_{eff}$  and  $\mu_{eff}$ ) are plotted to explain the absorption mechanism. It is further analyzed by plotting surface current density at all the five peak absorption frequencies. Polarization sensitivity of the structure is analyzed by simulated absorptivity response for both TE and TM polarizations. The proposed MA is fabricated, and scattering parameter is measured in an anechoic chamber with the help of vector network analyzer. Measured results approximately matched with the respective simulated ones within the tolerance limit. The proposed absorber is compared with already reported multiband absorbers. It has the highest number of absorption peaks and hexagonal packing with comparable unit cell size and thickness. With nearly 3% of FBW (at four absorption peaks) it can be used for many applications such as antenna, phase imaging, photo-detector, hyper-spectral imaging, micro-bolometer, spectroscopic detection, surveillance radar and other defence applications.

## REFERENCES

1. Smith, D. R., W. J. Padilla, D. C. Vier, S. C. Nemat-Nasser, and S. Schultz, "Composite medium with simultaneously negative permeability and permittivity," *Physical Review Letters*, Vol. 84, No. 18, 4184, May 1, 2000.
2. Alù, A. and N. Engheta, "Dispersion characteristics of metamaterial cloaking structures," *Electromagnetics*, Vol. 28, No. 7, 464–475, Sep. 25, 2008.
3. Zhao, Y. J., B. C. Zhou, Z. K. Zhang, R. Zhang, and B. Y. Li, "A compact tunable metamaterial filter based on split-ring resonators," *Optoelectronics Letters*, Vol. 13, No. 2, 120–122, Mar. 1, 2017.
4. Majid, H. A., M. K. Abd Rahim, and T. Masri, "Microstrip antenna's gain enhancement using left-handed metamaterial structure," *Progress In Electromagnetics Research M*, Vol. 8, 235–247, 2009.
5. Landy, N. I., S. Sajuyigbe, J. J. Mock, D. R. Smith, and W. J. Padilla, "Perfect metamaterial absorber," *Physical Review Letters*, Vol. 100, No. 20, 207402, May 21, 2008.
6. Li, M., H.-L. Yang, X.-W. Hou, Y. Tian, and D.-Y. Hou, "Perfect metamaterial absorber with dual bands," *Progress In Electromagnetics Research*, Vol. 108, 37–49, 2010.
7. Ramya, S. and I. S. Rao, "Design of polarization-insensitive dual band metamaterial absorber," *Progress In Electromagnetics Research M*, Vol. 50, 23–31, 2016.
8. Kaur, K. P., T. K. Upadhyaya, and M. Palandoken, "Dual-band polarization-insensitive metamaterial inspired microwave absorber for LTE-band applications," *Progress In Electromagnetics Research C*, Vol. 77, 91–100, 2017.
9. Khusboo, K., N. Mishra, and R. K. Chaudhary, "Wide-angle polarization independent triple band absorber based on metamaterial structure for microwave frequency applications," *Progress In Electromagnetics Research C*, Vol. 76, 119–127, 2017.
10. Zhai, H., C. Zhan, L. Liu, and C. Liang, "A new tunable dual-band metamaterial absorber with wide-angle TE and TM polarization stability," *Journal of Electromagnetic Waves and Applications*, Vol. 29, No. 6, 774–785, Apr. 13, 2015.
11. Ayop, O. B., M. K. Abd Rahim, N. A. Murad, N. A. Samsuri, and R. Dewan, "Triple band circular ring-shaped metamaterial absorber for X-band applications," *Progress In Electromagnetics Research M*, Vol. 39, 65–75, 2014.

12. Lu, L., S. Qu, H. Ma, F. Yu, S. Xia, Z. Xu, and P. Bai, "A polarization-independent wide-angle dual directional absorption metamaterial absorber," *Progress In Electromagnetics Research M*, Vol. 27, 91–201, 2012.
13. Luo, H. and Y. Z. Cheng, "Ultra-thin dual-band polarization-insensitive and wide-angle perfect metamaterial absorber based on a single circular sector resonator structure," *Journal of Electronic Materials*, Vol. 47, No. 1, 323–328, 2018.
14. Bhattacharyya, S., S. Ghosh, and K. Vaibhav Srivastava, "Triple band polarization-independent metamaterial absorber with bandwidth enhancement at X-band," *Journal of Applied Physics*, Vol. 114, No. 9, 094514, Sep. 7, 2013.
15. Chaurasiya, D., S. Ghosh, S. Bhattacharyya, and K. V. Srivastava, "An ultrathin quadband polarization-insensitive wide-angle metamaterial absorber," *Microwave and Optical Technology Letters*, Vol. 57, No. 3, 697–702, Mar. 1, 2015.
16. Zheng, D., Y. Cheng, D. Cheng, Y. Nie, and R. Z. Gong, "Four-band polarization-insensitive metamaterial absorber based on flower-shaped structures," *Progress In Electromagnetics Research*, Vol. 142, 221–229, 2013.
17. Wang, W., M. Yan, Y. Pang, J. Wang, H. Ma, S. Qua, H. Chen, C. Xu, and M. Feng, "Ultra-thin quadri-band metamaterial absorber based on spiral structure," *Applied Physics A*, Vol. 118, No. 2, 443–447, Feb. 1, 2015.
18. Mao, Z., S. Liu, B. Bian, B. Wang, B. Ma, L. Chen, and J. Xu, "Multi-band polarization-insensitive metamaterial absorber based on Chinese ancient coin-shaped structures," *Journal of Applied Physics*, Vol. 115, No. 20, 204505, May 28, 2014.
19. Smith, D. R., D. C. Vier, T. Koschny, and C. M. Soukoulis, "Electromagnetic parameter retrieval from inhomogeneous metamaterials," *Physical Review E*, Vol. 71, No. 3, 036617, Mar. 22, 2005.